nature cell biology

# Microtubule-dependent microtubule nucleation based on recruitment of γ-tubulin in higher plants

Takashi Murata[1,2,9], Seiji Sonobe[3], Tobias I. Baskin[4], Susumu Hyodo[5], Seiichiro Hasezawa[6], Toshiyuki Nagata[7], Tetsuya Horio[8] and Mitsuyasu Hasebe[1,2]

**Despite the absence of a conspicuous microtubule-organizing centre, microtubules in plant cells at interphase are present in the cell cortex as a well oriented array[1,2]. A recent report suggests that microtubule nucleation sites for the array are capable of associating with and dissociating from the cortex[3]. Here, we show that nucleation requires extant cortical microtubules, onto which cytosolic γ-tubulin is recruited. In both living cells and the cell-free system, microtubules are nucleated as branches on the extant cortical microtubules. The branch points contain γ-tubulin, which is abundant in the cytoplasm, and microtubule nucleation in the cell-free system is prevented by inhibiting γ-tubulin function with a specific antibody. When isolated plasma membrane with microtubules is exposed to purified neuro-tubulin, no microtubules are nucleated. However, when the membrane is exposed to a cytosolic extract, γ-tubulin binds microtubules on the membrane, and after a subsequent incubation in neuro-tubulin, microtubules are nucleated on the pre-existing microtubules. We propose that a cytoplasmic γ-tubulin complex shuttles between the cytoplasm and the side of a cortical microtubule, and has nucleation activity only when bound to the microtubule.**

Almost all microtubule arrays are organized by one or more microtubule-organizing centres, such as centrosomes, that regulate nucleation spatially and temporally[4]. It has long been puzzling how, despite the absence of conspicuous organizing centres, higher plant cells form well-organized cortical microtubule arrays, which are essential for cell morphogenesis[1,2]. On the basis of Mazia's hypothesis of a diffuse centrosome[5], microtubules in the cortical array are widely assumed to be formed by nucleation sites dispersed along the plasma membrane[2,6]. AtEB1a–GFP has been used as a marker for microtubule nucleation and, consistent with Mazia's hypothesis, the signal associates with and dissociates from the cortex, rather than being fixed in place[3].

An alternative model, in which microtubules themselves participate in the deployment of their nucleation sites, was made in a pioneering study of reassembly after drug-induced depolymerization in internodal cells of *Nitella tasmanica*, a charalean alga[7]. Based on the fact that microtubules reappeared during reassembly in the form of highly branched clusters, and because the cortical array of untreated cells included branched microtubules, the authors hypothesized that nucleation sites are recruited by extant microtubules[7]. Recently, a similar pattern of microtubule-dependent microtubule nucleation was discovered in fission yeast, although here the nucleated microtubules form a bundle without branching[8]. Microtubule initiation through branching on an existing microtubule has been imaged directly in living cells of the model flowering plant *Arabidopsis thaliana*[9,10]; however, microtubule initiation at cortical sites without an existing microtubule was also seen. Therefore, although microtubule-dependent microtubule nucleation seems to occur among cortical microtubules, it is not clear to what extent this mode of microtubule assembly contributes to the formation and maintenance of the cortical array.

Whether microtubule-dependent or not, the molecular character of the cortical nucleating material is unknown. Although AtEB1a–GFP labels spindle poles[3], it is unclear whether native AtEB1 protein localizes to cortical nucleation sites[11,12]. It is accepted that γ-tubulin is responsible, as part of a complex[13], for nucleation within microtubule-organizing centres[4]. In higher plant cells at interphase, γ-tubulin localizes mainly to the cytoplasm[6,14,15], and localization to the cortical array has also been reported[14,16,17]. On the basis of cytoplasmic localization of γ-tubulin, recruitment of γ-tubulin complexes from the cytoplasm to the cortex has been proposed[6]. Involvement of γ-tubulin in the branching of microtubules has also been predicted[1]. However, no data have been reported demonstrating the activity of this protein in nucleating cortical microtubules[1,2,6].

Here, we show that microtubule-dependent microtubule nucleation is the predominant pathway of microtubule nucleation for the cortical

[1]National Institute for Basic Biology, Okazaki 444-8585, Japan. [2]The Graduate University for Advanced Studies, Hayama, Kanagawa 240-0193, Japan. [3]Graduate School of Life Science, University of Hyogo, Hyogo 678-1297, Japan. [4]Biology Department, University of Massachusetts, Amherst, MA 01003, USA. [5]Ocean Research Institute, The University of Tokyo, Tokyo 164-8639, Japan. [6]Department of Integrated Biosciences, Graduate School of Frontier Sciences, The University of Tokyo, Chiba 277-8562, Japan. [7]Department of Biological Sciences, Graduate School of Science, The University of Tokyo, Tokyo 113-0033, Japan. [8]Institute of Health Biosciences, University of Tokushima Graduate School, Tokushima 770-8503, Japan.
[9]Correspondence should be addressed to T.M. (e-mail: tkmurata@nibb.ac.jp)

Received 29 June 2005; accepted 12 August 2005; published online: 4 September 2005; DOI: 10.1038/ncb1306

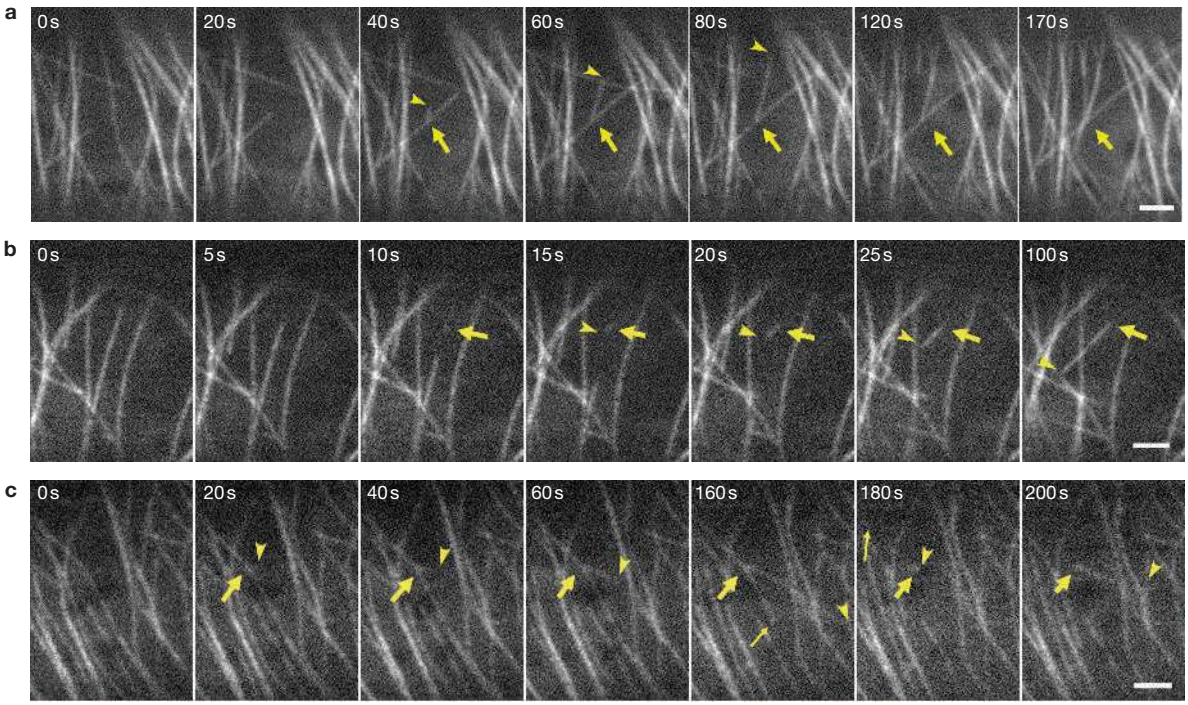


**Figure 1** Initiation of cortical microtubules as branches in tobacco cells. (**a**) Branching from an elongating microtubule. (**b**) Microtubule initiation immediately following depolymerization of the original microtubule. (**c**) Depolymerization of the original microtubule after branching. Branch vertices (thick arrows), the ends of newly initiated microtubules (arrowheads), and the end of an original microtubule (**c**; thin arrows) are shown. Scale bars, 2 μm.

array, and that cytosolic γ-tubulin binds to existing cortical microtubules and nucleates new microtubules as branches.

To address the role of extant microtubules in microtubule nucleation within the cortical array, we examined tobacco suspension culture cells expressing GFP–α-tubulin[18] using time-lapse imaging. We found that most microtubules (69 out of 77) were initiated on extant microtubules (Fig. 1a; see Supplementary Information, Movie S1), forming a branched structure. Notably, all of the eight microtubules that scored as initiating without an extant microtubule formed at a site where a microtubule had disappeared no more than 15 s earlier (Fig. 1b; see Supplementary Information, Movie S2). A few microtubules emerged from a bundle of existing microtubules and were not counted. After formation, the branched structure was often lost by depolymerization of the original microtubule (Fig. 1c; see Supplementary Information, Movie S3) or hidden by polymerization of other microtubules (Fig. 1a; see Supplementary Information, Movie S1).

After depolymerization of the 'original' microtubule, the microtubule end at the initiation site (the presumptive minus end) remained stable, whereas the microtubule end that had grown from the initiation site (the presumptive plus end) repeatedly grew and shrank. The presumptive plus end sometimes depolymerized completely, but then a second microtubule would appear to regrow from the first microtubule's initiation site (Fig. 1c; see Supplementary Information, Movie S3). To account for such behaviour, we conclude that microtubule-independent initiation, if it exists at all, rarely contributes to the formation of microtubules in the cortical array. Consistently, initiation of microtubules on extant microtubules predominates in leaf epidermal cells of *A. thaliana* expressing GFP–α-tubulin (see Supplementary Information, Movie S4).

The angle of branching — that is, the angle between the original microtubule and the newly formed microtubule — was well defined (41.6 ± 8.2 °), suggesting a physical connection between the original microtubule and the minus end of the new one. Initiation of microtubules parallel to the original microtubules, as recently seen in fission yeast[8], was not detected (data not shown). Among the cases in which the original microtubule disappeared just before microtubule initiation, the apparent angle of branching was more variable (for example, Fig. 1b), perhaps indicating the loss of a stabilizing effect from the branch point.

To evaluate the functional role of microtubules in nucleation, we used a previously developed cell-free system[19] in which microtubule polymerization is obtained by incubating plasma-membrane ghosts (Fig. 2a) in a cytosolic extract that contains endogenous tubulin. We distinguished the microtubules that were originally present in the ghosts from those that polymerized during incubation, by adding a small amount of rhodamine-labelled brain tubulin (0.1 mg $ml^{-1}$, final concentration) to the extract. After incubation and fixation, all microtubules were detected immunologically whereas only the newly assembled ones contained rhodamine. After 2 min of incubation, microtubule density had increased modestly and after 10 min the increase was substantial (see Supplementary Information, Fig. S1). Polymerization of tubulin within the extract in the absence of ghosts was not detected (data not shown). The newly assembled microtubules appeared to extend from the original ghost microtubules at branch points (Fig. 2b; left), forming tree-like structures (Fig. 2b; right). Initiation of microtubules on the side of microtubules was confirmed by electron microscopy (Fig. 2c). The angle between arms of the branch was well defined (36.0 ±10.7 °), and indistinguishable in the cell-free system and living cells (Fig. 2d). The similarity of the angular distributions suggests that microtubule initiation in living cells and in the cell-free system is accomplished by the same mechanism.

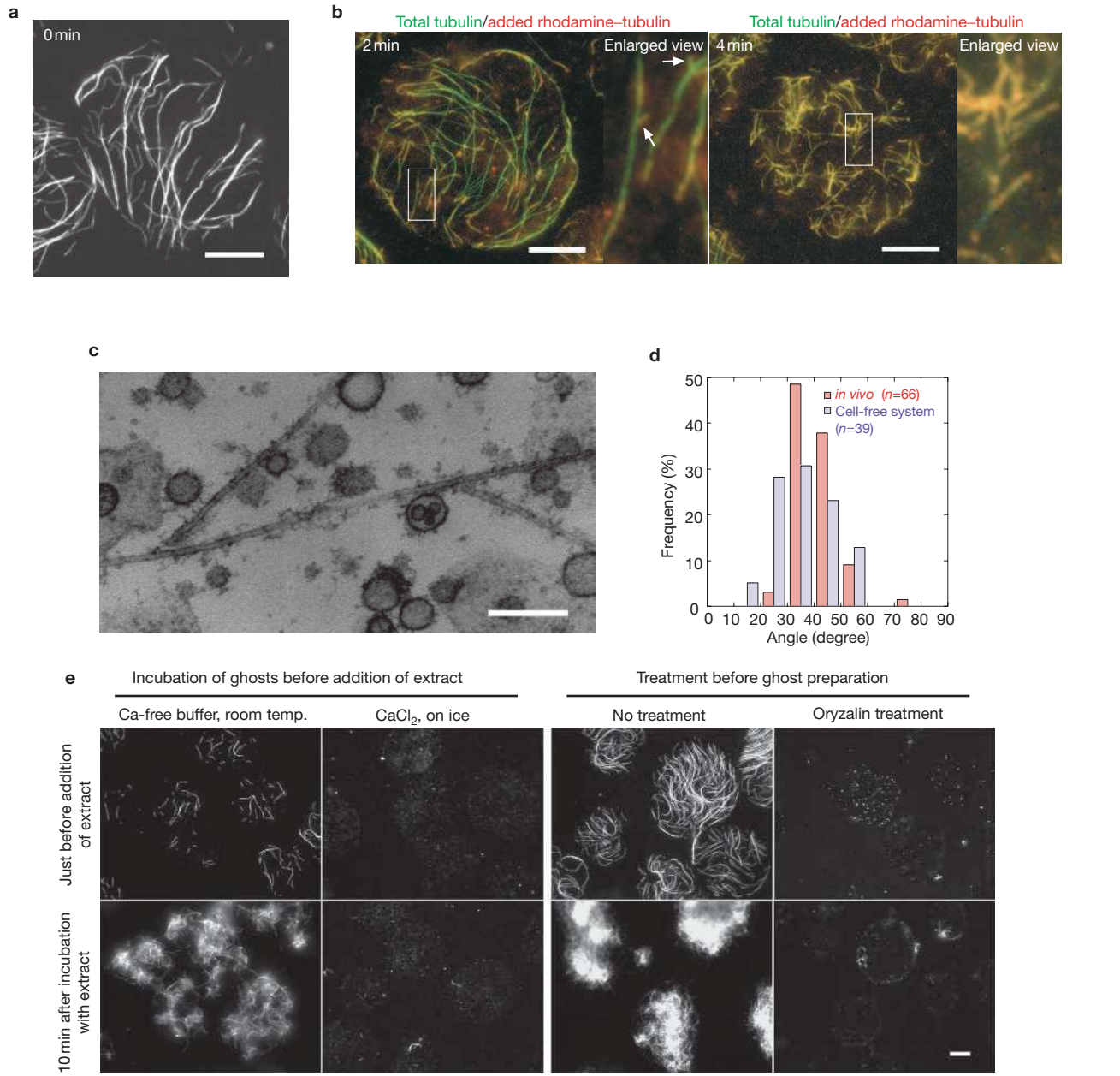


**Figure 2** Extant microtubules are essential for microtubule assembly in the cell-free system. (**a**) Ghost microtubules before assay. (**b**) Microtubule assembly upon incubation with a cytosolic extract. Images of total tubulin and added rhodamine–tubulin. Microtubule branches labelled by rhodamine–tubulin are shown. Arrows, branched microtubules at 2 min. (**c**) Transmission electron micrograph of a ghost 3 min after extract treatment. (**d**) Branch angles in living cells and the cell-free system. (**e**) Inhibition of microtubule assembly by removal of ghost microtubules. Scale bars, 10 μm (**a**, **b**, **e**) and 200 nm (**c**).

We tested the role of extant microtubules in microtubule nucleation by removing microtubules before the assay (Fig. 2e). When ghosts were incubated for 1 h in calcium-free buffer at room temperature, the remaining ghost microtubules were capable of seeding microtubule assembly; however, when the ghosts were chilled in the presence of calcium for 1 h, ghost microtubules were completely depolymerized, and upon subsequent incubation in the extract under control conditions, microtubules failed to assemble. Likewise, when ghosts without microtubules were prepared by treating protoplasts before lysis with the anti-microtubule reagent, oryzalin, assembly was inhibited. Our experiments indicate that a microtubule-dependent pathway is essential for nucleation of microtubules on the ghost plasma membrane.

Next, we characterized microtubule initiation further by examining the role of γ-tubulin. To investigate the role of γ-tubulin in microtubule-dependent microtubule nucleation, we raised an antibody against the carboxyl terminal of tobacco γ-tubulin (see Supplementary Information, Fig. S2). Similar to a previous report[6], diffuse staining was seen throughout the cytoplasm by immunofluorescence microscopy (Fig. 3a). Occasionally, weak and punctate γ-tubulin labelling was seen at the branch points of cortical microtubules by confocal laser scanning microscopy, but labelling was also seen in the cytoplasm (Fig. 3b). To localize γ-tubulin within the cortical array, we used immunogold and electron microscopy. Freshly isolated ghosts were immediately fixed, labelled with the anti-γ-tubulin antibody and a gold-conjugated

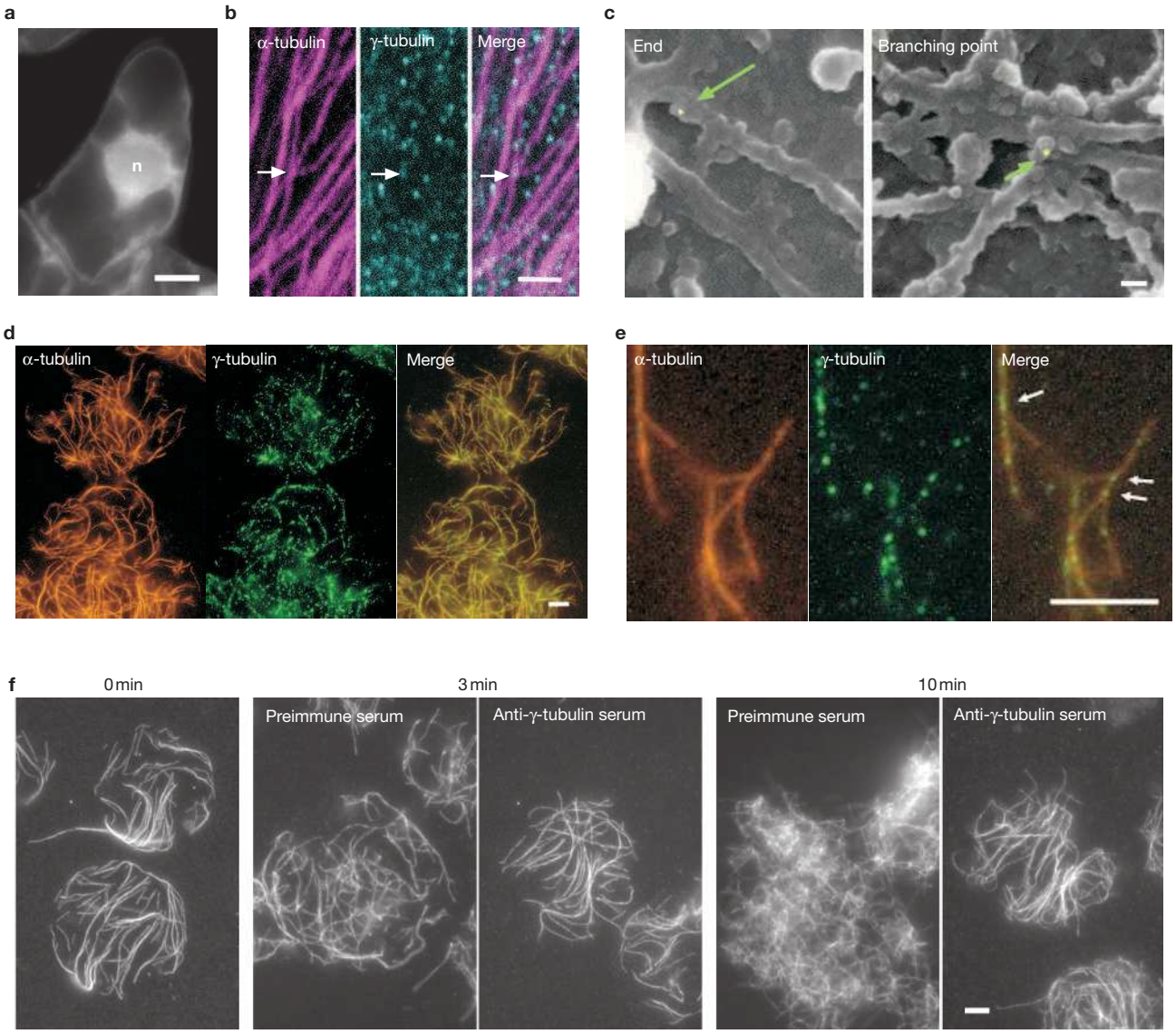


**Figure 3** γ-tubulin is essential for microtubule nucleation on microtubules. (**a**) Tobacco BY-2 cell labelled with anti-γ-tubulin. n, nucleus. (**b**) Confocal micrographs of the cell cortex showing α- and γ-tubulin localization and their overlap at a branch vertex (arrows). (**c**) Field-emission scanning electron micrographs of ghosts labelled with anti-γ-tubulin (yellow, arrows). (**d**, **e**) Localization of α- and γ-tubulin in the cell-free system 3 min after extract treatment. γ-tubulin labelling at branch points (**e**; arrows) is shown. (**f**) Inhibition of microtubule assembly by anti-γ-tubulin serum. Scale bars, 10 μm (**a**), 2 μm (**b**), 50 nm (**c**) and 5 μm (**d**–**f**).

secondary antibody, and observed by field-emission scanning electron microscopy[20]. In ghosts from which the cytoplasm had been mostly removed, 18 out of 54 gold particles were localized at the end (including the branching point) of a microtubule (Fig. 3c), 3 out of 54 were localized at the side of a microtubule, and the remaining gold particles labelled uncharacterized material (data not shown). Localization of gold particles at the ends of microtubules was reproduced by another lot of the antibody, for which the final adsorption step of purification was omitted (see Supplementary Information, Table S1). Among the particles at microtubule ends from both preparations, 11 out of 40 were at branch points (Fig. 3c; right). Given that γ-tubulin is localized at cortical branch points, we hypothesize that γ-tubulin is involved in the initiation of microtubules at the sides of extant microtubules. The fact that γ-tubulin localized to some free microtubule ends (Fig. 3c; left) is consistent with the observation in living cells that the original microtubules frequently depolymerize (Fig. 1c).

To examine the requirement for γ-tubulin in microtubule assembly, we used the cell-free system. Before adding cytosolic extract, γ-tubulin was rarely detected on the microtubules (Fig. 3c; see also left-most panel in Fig. 4b). After adding extract, γ-tubulin-labelled ghost microtubules were common (Fig. 3d), with labelling present at branch sites (Fig. 3e). Consistent with the γ-tubulin localization, addition of the anti-γ-tubulin antiserum to the cytosolic extract inhibited branch formation (3 min in Fig. 3f) and microtubule assembly (10 min in Fig. 3f).

To further determine whether γ-tubulin binding to extant microtubules is necessary for the formation of new ones, we developed a sequential treatment system using purified tubulin. Ghosts were incubated in a cytosolic extract treated with oryzalin, which binds to and inactivates plant αβ-tubulin, and then the treated ghosts were incubated in purified neural αβ-tubulin (Fig. 4a). Ghosts that were incubated directly in the neural tubulin nucleated few microtubules (Fig. 4b; left). However, when

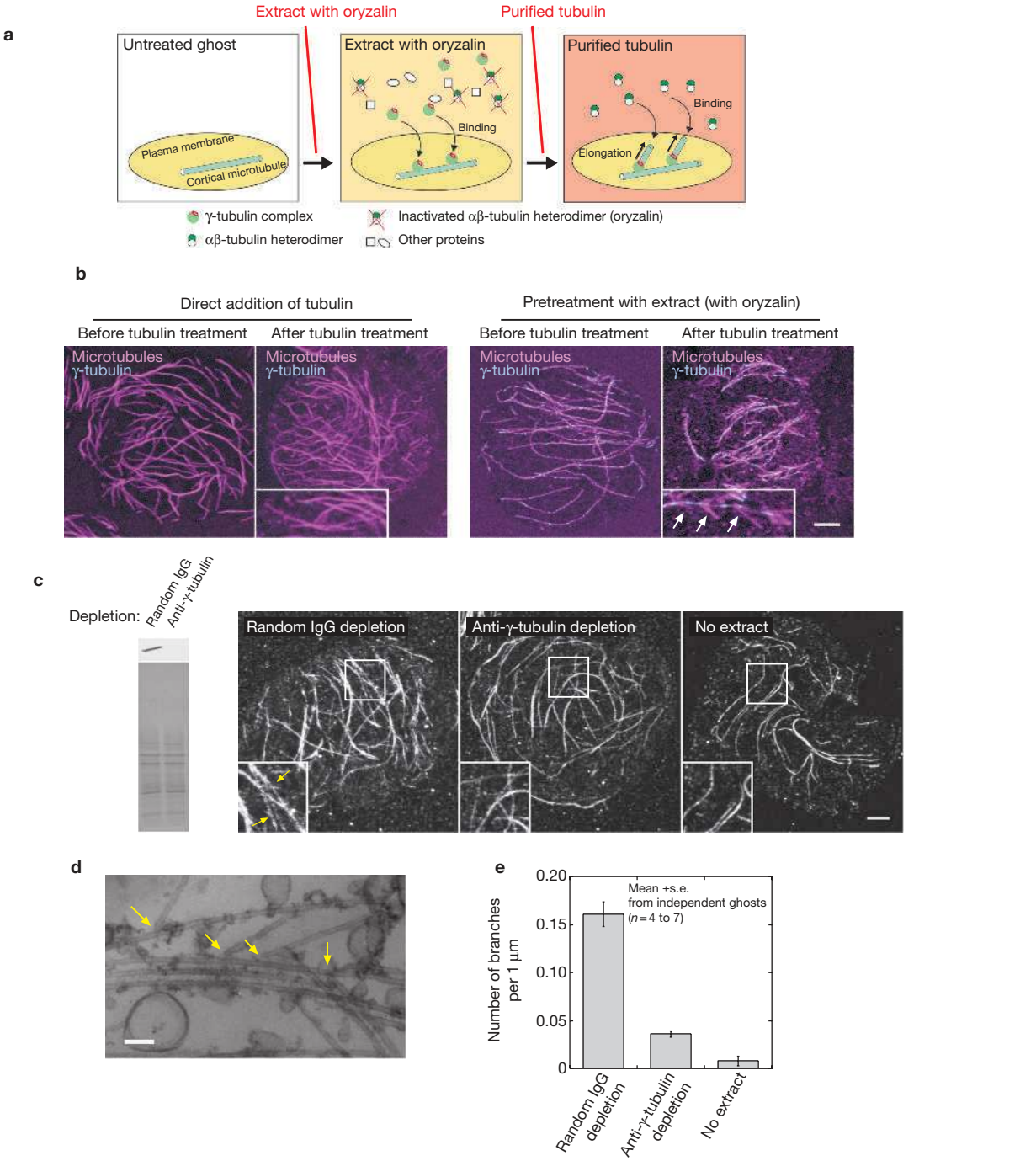


**Figure 4** Recruitment of cytosolic γ-tubulin for microtubule nucleation. (**a**) Diagram of the assay. (**b**) Cytosolic extract supports subsequent assembly of neuro-tubulin. Merged images of microtubules and γ-tubulin. Insets show presence or absence of branch formation (arrows) at high magnification. (**c**) Effects of γ-tubulin depletion on assembly of tobacco tubulin. Immunoblots with corresponding gels (left) and α-tubulin images in ghosts (right) are shown. Insets are enlarged views of the boxed regions, indicating branched structure of microtubules (arrows). (**d**) Electron micrograph of a ghost from random IgG depletion in **c**. Arrows indicate the branched structure of microtubules. (**e**) Frequency of branched microtubules. Scale bars, 4 μm (**b**, **c**) and 100 nm (**d**).

ghosts that were incubated in oryzalin-treated extract were subsequently exposed to the neuro-tubulin, microtubules formed abundantly as typical branched structures (Fig. 4b; right), although pre-existing microtubules did not elongate because of the oryzalin treatment[6]. The oryzalin-treated extract led to profuse labelling of the pre-existing microtubules with γ-tubulin (Fig. 4b; right), which appeared at branch foci following neuro-tubulin treatment (Fig. 4b; inset). That the cytosolic extract conferred microtubule-nucleation activity to the ghosts was confirmed by repeating these experiments with tubulin that was purified from tobacco BY-2 cells[21] instead of neuro-tubulin, and with the inhibitor propyzamide, which has better reversibility than oryzalin. Assays with plant tubulin and propyzamide gave results similar to those shown in Fig. 4b (see Supplementary Information, Fig. S3).

The role of γ-tubulin in the system was examined further by immunodepletion. When γ-tubulin was depleted from the propyzamide-treated extract (see Supplementary Information, Fig. S4), the number of

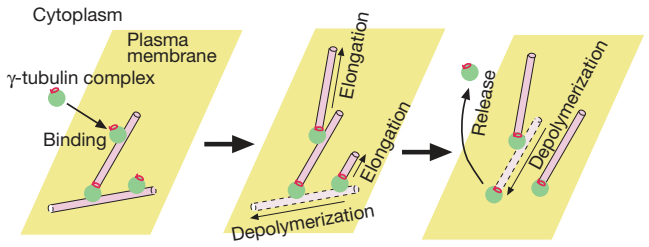


**Figure 5** Model for nucleation of cortical microtubules in plants. Cytosolic γ-tubulin complexes bind onto pre-existing cortical microtubules (left) and nucleate microtubules as branches (centre). The original microtubules frequently depolymerize (centre) but γ-tubulin complexes are not released until depolymerization of newly formed microtubules occurs (right).

subsequently formed, branched microtubules was reduced (Fig. 4c). We quantified microtubule assembly in this system by electron microscopy, through which individual branches could be resolved clearly (Fig. 4d). The number of branch points per unit length of microtubule was reduced by depletion of γ-tubulin (Fig. 4e; see Supplementary Information, Fig. S5). In the cell-free system, cytosolic γ-tubulin is evidently essential for microtubule nucleation as branches.

Overall, we conclude that in higher plants cortical microtubules are nucleated by γ-tubulin recruited from the cytosol to the sides of previously formed microtubules. We propose that a γ-tubulin complex shuttles between the cytosol and the side of a cortical microtubule, being active for nucleation while bound to the microtubule, and being released to the cytosol when the original microtubule depolymerizes (Fig. 5).

We show that microtubule-dependent microtubule nucleation is essential for assembly of microtubules in the cortical array. In previous reports, *de novo* formation of microtubules without pre-existing microtubules has been reported[9,10]. We argue that such microtubule nucleation is likely to be derived from sites on existing microtubules because we saw that the nucleated microtubule can grow and shrink extensively after depolymerization of the original microtubule (Fig. 1c). After depolymerization of both microtubules of a branch, the microtubule nucleating complex may weakly bind to the cell cortex; while it remains bound, a nucleation event could occur.

From our results it is paradoxical that microtubules in the cortical array mostly run parallel to each other, but microtubules nucleate as branches diverging by approximately 40 ° from the original orientation (Fig. 2d). To maintain the parallel organization, nascent microtubules might be realigned or removed. Microtubule removal has been indicated by cell lysis experiments in which cortical microtubule half-life was shown to be a function of orientation[22]. Microtubule realignment has been indicated by observations in living cells of bundle formation[10]. Interestingly, the fate of a growing microtubule is influenced by the angle at which it encounters another microtubule[23]: at steep angles, the microtubule tends to depolymerize, whereas at shallow angles the microtubule tends to be captured and grow parallel to the encountered one forming a bundle. Intriguingly, the cut-off between steep and shallow angles is approximately 40 °, the same as was found here for nucleation. For parallel microtubules, the observed angle for nucleation is the maximal angle for divergence to avoid catastrophic collisions. Diverging nucleation and convergent capture may permit the cortical array to place microtubules throughout the cortex as well as having the microtubules run parallel.

We show here that cytosolic γ-tubulin is essential for microtubule nucleation on extant microtubules. To our knowledge, this is the first identification of any protein as being essential for microtubule nucleation within the plant cortical array. The role of γ-tubulin in nucleation of cortical microtubules has been enigmatic, in part because γ-tubulin does not localize preferentially to the ends of the cortical microtubules[6,15,16,24,25]. Our finding that cytoplasmic γ-tubulin binds to the side of a microtubule upon a nucleation event explains γ-tubulin being localized both in the cytoplasm[6,15] and at the sides of microtubules[16,17,25]. To address the molecular mechanisms of γ-tubulin recruitment and microtubule-dependent microtubule nucleation, it will be essential to characterize the components of the plant γ-tubulin complex and define their interactions.

In the plant mitotic spindle and cytokinetic phragmoplast, branched microtubules, called fir trees or converging centres, have been observed frequently[26–28]. Hence, microtubule-dependent microtubule nucleation, mediated by γ-tubulin, may have a role in microtubule nucleation for these arrays. In plant cells, which generally lack conspicuous organizing centres, analysis of the role of γ-tubulin in organizing the spindle and phragmoplast might reveal a ubiquitous role for microtubule-dependent microtubule nucleation. □

## METHODS

**Cells.** Tobacco BY-2 cells and BYGT16 cells expressing GFP–α-tubulin[18] were cultured as described elsewhere[29]. Cells at stationary phase (7 days after subculture) were used for live imaging of microtubules. Plasma membrane ghosts and cytosolic extract were isolated from cells 5 days after subculture[19]. Seeds of *A. thaliana* expressing GFP–α-tubulin[30] were kindly provided by T. Hashimoto (Nara Institute of Science and Technology). Plants of *gl1* background, without development of trichomes, were used.

**Antibodies.** Rabbit serum against a C-terminal peptide of tobacco γ-tubulin (DHVLTGEGNASGTVDPKLSL) and an affinity-purified antiserum against the antigen peptide were prepared by Sawady Technology Co. (Tokyo, Japan). For immunofluorescence, the affinity-purified antibody was further purified by adsorption with tobacco proteins separated by SDS-polyacrylamide gel electrophoresis (relative molecular masses ($M_r$) of 60K–80K) after dilution with phosphate-buffered saline, because the affinity-purified antibody reacted with proteins of $M_r$ ~75K on a western blot (in addition to tobacco γ-tubulin; $M_r$ ~55K). The specificity of the purified antibody against tobacco proteins was confirmed by immunoblotting (see Supplementary Information, Fig. S2). A monoclonal antibody against fission yeast γ-tubulin (clone G9)[31] was also used to detect γ-tubulin in the cytosolic extract. Specific binding of the monoclonal antibody was confirmed by immunoblotting (see Supplementary Information, Fig. S2).

**Live imaging of microtubules.** Tobacco cells expressing GFP–α-tubulin were observed through an inverted microscope equipped with a spinning disc confocal unit (Yokogawa CSU21; Musashino, Japan) and a cooled CCD camera (CoolSNAP HQ; Nippon Roper, Chiba, Japan). A suspension of cells was mounted on a glass slide with a coverslip (22 × 22 mm$^2$). Two sides of the coverslip were sealed with silicon grease and the remaining two sides were left open. Cells were alive for at least 3 h, and the positions of cells were fixed because of the high density of cells. Images (48 × 34 μm$^2$) of the cell cortex were captured at 5-s intervals. We observed 83 cells over a total period of 909 min. Epidermal cells of *A. thaliana* were observed using the same system as described above. Cells of the second true leaves of seedlings were used.

**Preparation of plasma membrane ghosts.** Five-day-old BY-2 cells were digested with 1% Cellulase Onozuka RS (Yakuruto Honsha Co., Tokyo, Japan) and 0.1% Pectolyase Y-23 (Seishin Pharmaceutical Co., Tokyo, Japan) in 0.5 M mannitol for 1.5 h, or with 2% Sumizyme (Shin Nihon Chemical Co., Anjo, Japan) and 0.2% Sumizyme AP-2 (Shin Nihon Chemical Co.) in 0.45 M sorbitol for 2.5 h. The released protoplasts were attached onto a poly-L-lysine-coated coverslip, and lysed by shaking in lysis buffer (50 mM PIPES, 5 mM EGTA, 2 mM $MgCl_2$ or 1 mM $MgSO_4$, pH 6.8). To obtain microtubule-free ghosts, protoplasts were isolated in the presence of 10 μM oryzalin or ghosts were incubated with lysis buffer supplemented

with calcium (50 mM PIPES, 1 mM calcium chloride, 2 mM $MgCl_2$, pH 6.8) for 1 h at room temperature. For field-emission scanning electron microscopy, the ghosts were prepared in the presence of 0.005% Nonidet P-40 and 10 μM taxol.

**Preparation of a cytosolic extract, cell-free system and immunodepletion of the extract.** Protoplasts were prepared from 5-day-old BY-2 cells pretreated with 3 mg $l^{-1}$ aphidicolin for 10–16 h. The protoplasts were centrifuged at 23,000*g* for 40 min in 0.6 M sorbitol that contained 36% Percoll (Amersham Biosciences, Uppsala, Sweden), 4 mM $MgCl_2$, pH 7.3. The resulting evacuolate protoplasts were gently homogenized by a glass homogenizer with one-half volume of extraction buffer (50 mM PIPES, 10 mM EGTA, 2 mM $MgCl_2$, 4 mM dithiothreitol, 15% sucrose) containing a protease inhibitor cocktail (Complete Mini EDTA-free; Roche Applied Science, Penzberg, Germany) on ice. The homogenate was centrifuged at 16,000*g* for 5 min, and the supernatant was further centrifuged at 39,000*g* for 20 min. The resulting clear supernatant was frozen in liquid nitrogen, stored at –80 °C; this was used as the cytosolic extract.

For assays, ghosts were incubated with cytosolic extract at 23–27 °C. To distinguish newly polymerized tubulin, 1/10 volume of 1 mg $ml^{-1}$ bovine brain tubulin, labelled with rhodamine (T331; Cytoskeleton Co., Denver, CO), was added to the extract in some cases. The addition of the labelled tubulin or addition of buffer did not affect the course of microtubule assembly as judged by immunofluorescence microscopy. To block polymerization of tubulin, oryzalin or propyzamide was added to the extract at a final concentration of 10 or 50 μM, respectively, and the extract was incubated for more than 30 min on ice prior to assay. For assembly of brain tubulin (T238; Cytoskeleton Co.), 1 mg $ml^{-1}$ tubulin (≥99% pure) was incubated at 32 °C. Tobacco tubulin was purified as described[21]. For assembly, 0.5 mg $ml^{-1}$ tubulin was incubated at 30 °C.

Immunodepletion was essentially the same as described previously[32]. For immunodepletion of the extract, the extract was diluted with the extraction buffer to obtain a protein concentration of 8 mg $ml^{-1}$, and propyzamide (50 μM final concentration) was added to the diluted extract. Protein A-sepharose beads (Amersham Biosciences) that were pre-incubated with 3.5 mg of affinity-purified anti-γ-tubulin or rabbit random IgG (PP64; Chemicon International, Temecula, CA) in TBS-TX (150 mM sodium chloride, 10 mM Tris, 0.1% Triton X-100, pH 7.5) were washed three times with extraction buffer. The diluted, propyzamide-treated extracts were incubated with the antibody beads at 4 °C for 2 h under gentle rotation (two inversions per minute). The beads were removed from the extract by centrifugation (10,000*g* for 5 s), and the extract was used for assay. In the protein fraction bound to the anti-γ-tubulin beads, western blotting with the unadsorbed anti-γ-tubulin antibody detected only γ-tubulin, indicating that non-specific binding did not occur during immunodepletion. Binding of γ-tubulin with the beads was confirmed by G9 monoclonal antibody (see Supplementary Information, Fig. S4).

**Immunofluorescence microscopy.** Five-day-old BY-2 cells were fixed in 3.7% formaldehyde and 0.08% glutaraldehyde dissolved in PME buffer (50 mM PIPES, 1 mM $MgSO_4$, 5 mM EGTA, pH 6.8) at room temperature for 1 h. Adding glutaraldehyde to a fixative greatly improved preservation of microtubules, although autofluorescence from nuclei increased (data not shown). The fixed cells were washed with PME buffer, attached onto polyethyleneimine-coated coverslips, and digested with enzyme solution, which contained 2% Driserase, 0.4 M mannitol and 0.1% Nonidet P-40 supplemented with protease inhibitor cocktail (Complete Mini EDTA-Free, Roche) for 10 min. The digested cells were treated with 1% Triton X-100 in PME buffer for 10 min, washed with phosphate-buffered saline, and incubated with the adsorption-purified antibody against tobacco γ-tubulin (1:500–1:1,000) followed by Alexa 488-labelled anti-mouse IgG (Molecular Probes, Eugene, OR).

For dual localization of microtubules and γ-tubulin in the cortical cytoplasm, 7-day-old BY-2 cells were fixed in 7.6% formaldehyde and 0.16% glutaraldehyde dissolved in PME buffer for 30 min. The fixed cells were sandwiched between polyethyleneimine-coated coverslips, frozen in liquid nitrogen and cleaved by splitting coverslips. The cleaved cells were thawed and blocked with a solution that contained 1% bovine serum albumin, 0.1% Nonidet P-40, and protease inhibitor (Complete Mini EDTA-free) dissolved in phosphate-buffered saline. The cells were incubated with a mixture of mouse monoclonal antibody against chicken brain tubulin (1:50–1:100; CP06; Oncogene Research Products, San Diego, CA) and the adsorption-purified antibody against tobacco γ-tubulin (1:500–1:1,000). The cells that were incubated with the primary antibody were washed with phosphate-buffered saline, and incubated with a mixture of Alexa 594-labelled anti-mouse IgG (1:500) and Alexa 488-labelled anti-rabbit IgG. (1:500). The labelled cells were observed by an epifluorescence microscope or a confocal microscope (TCS SP2; Leica).

Plasma membrane ghosts treated with or without cytosolic extract were fixed in 3.7% formaldehyde and 0.08% glutaraldehyde dissolved in PME buffer (50 mM PIPES, 1 mM $MgSO_4$, 5 mM EGTA, pH 6.8) at room temperature for 1–2 h. The fixed ghosts were washed with phosphate-buffered saline, and labelled with the primary and the secondary antibodies as above. For dual labelling of α-tubulin and γ-tubulin, Alexa 546- or Alexa 633-labelled anti-rabbit IgG (Molecular Probes) were used as the secondary antibody, instead of Alexa 594-labelled anti-rabbit IgG.

**Field-emission scanning electron microscopy.** Plasma-membrane ghosts were fixed with 0.1% glutaraldehyde and 0.5% paraformaldehyde in PME buffer for 30 min. The fixed ghosts were blocked with 1% bovine serum albumin for 2 h, and incubated with the purified anti-tobacco γ-tubulin (1:250) for 2 h. After washing with phosphate-buffered saline, the ghosts were labelled with anti-rabbit IgG conjugated with 10-nm colloidal gold (Electron Microscopy Sciences, Hatfield, PA) diluted 1:30 for 2 h. The labelled ghosts were washed with phosphate-buffered saline, postfixed with 0.5% osmium tetroxide, dehydrated in a graded ethanol series and critical-point dried. The preparations were coated with carbon and observed with a field scanning electron microscope (Hitachi S-4700, Tokyo, Japan) at 5 KV. Localization was studied in overlays of the secondary electron signal (grey in Fig. 3c) and the back-scattered electron signal, which showed immunogold at high contrast (yellow in Fig. 3c).

**Transmission electron microscopy.** Ghosts prepared on a plastic sheet (Cat. No. 160-08893; Wako Pure Chemical Industries, Osaka, Japan) were treated with cytosolic extract for 3 min and fixed with 2.5% glutaraldehyde in 0.1 M sodium phosphate buffer containing 5 mM EGTA for 2 h at room temperature. The fixed ghosts were washed with 0.1 M sodium phosphate buffer chilled on ice, and postfixed with 1% aqueous osmium tetroxide for 3 h on ice. The ghosts were then dehydrated with acetone, and embedded with Epon resin. After removal of the plastic sheet, the embedded ghosts were sectioned parallel to the plane of the plastic sheet. The sections were stained with uranyl acetate followed by lead citrate, and observed with an electron microscope (JEOL 1200EX, JEOL, Akishima, Japan) at 80 KV.

*Note: Supplementary information is available on the Nature Cell Biology website.*

ACKNOWLEDGEMENTS

We greatly acknowledge T. Hashimoto for providing the GFP–tubulin line. We thank P. Wadsworth for incisive comments on the manuscript. Field-emission scanning electron microscopy was done at the University of Missouri's Core Facility for Electron Microscopy and we thank R. Johnson for his help there. This work was supported by grant-in-aids from Japan Society for the Promotion of Science and Ministry of Education, Culture, Sports, Science and Technology to T.M. and M.H., and in part by a grant to T.I.B. from the US Department of Energy (award No. 03ER15421).

COMPETING FINANCIAL INTERESTS

The authors declare that they have no competing financial interests.

Published online at http://www.nature.com/naturecellbiology/
Reprints and permissions information is available online at http://npg.nature.com/reprintsandpermissions/

1. Wasteneys, G. O. Microtubule organization in the green kingdom: chaos or self-order? *J. Cell Sci.* **115,** 1345–1354 (2002).
2. Lloyd, C. W. & Chan, J. Microtubules and the shape of plants to come. *Nature Rev. Mol. Cell Biol.* **5,** 13–22 (2004).
3. Chan, J., Calder, G. M., Doonan, J. H. & Lloyd, C. W. EB1 reveals mobile microtubule nucleation sites in *Arabidopsis*. *Nature Cell Biol.* **5,** 967–971 (2003).
4. Job, D., Valiron, O. & Oakley, B. Microtubule nucleation. *Curr. Opin. Cell Biol.* **15,** 111–117 (2003).
5. Mazia, D. Centrosomes and mitotic poles. *Exp. Cell Res.* **153,** 1–15 (1984).
6. Erhardt, M. *et al.* The plant Spc98p homologue colocalizes with γ-tubulin at microtubule nucleation sites and is required for microtubule nucleation. *J. Cell Sci.* **115,** 2423–2431 (2002).
7. Wasteneys, G. O. & Williamson, R. E. Reassembly of microtubules in *Nitella tasmanica* - Assembly of cortical microtubules in branching clusters and its relevance to steady-state microtubule assembly. *J. Cell Sci.* **93,** 705–714 (1989).
8. Janson, M. E., Setty, T. G., Paoletti, A. & Tran, P. T. Efficient formation of bipolar microtubule bundles requires microtubule-bound γ-tubulin complexes. *J. Cell Biol.* **169,** 297–308 (2005).

9. Van Bruaene, N., Joss, G. & Van Oostveldt, P. Reorganization and *in vivo* dynamics of microtubules during *Arabidopsis* root hair development. *Plant Physiol.* **136,** 3905–3919 (2004).
10. Shaw, S. L., Kamyar, R. & Ehrhardt, D. W. Sustained microtubule treadmilling in *Arabidopsis* cortical arrays. *Science* **300,** 1715–1718 (2003).
11. Sedbrook, J. C. MAPs in plant cells: delineating microtubule growth dynamics and organization. *Curr. Opin. Plant Biol.* **7,** 632–640 (2004).
12. Bisgrove, S. R., Hable, W. E. & Kropf, D. L. +TIPs and microtubule regulation. The beginning of the plus end in plants. *Plant Physiol.* **136,** 3855–3863 (2004).
13. Zheng, Y., Wong, M. L., Alberts, B. & Mitchison, T. Nucleation of microtubule assembly by a γ-tubulin-containing ring complex. *Nature* **378,** 578–583 (1995).
14. Liu, B., Marc, J., Joshi, H. C. & Palevitz, B. A. A γ-tubulin-related protein associated with the microtubule arrays of higher plants in a cell cycle-dependent manner. *J. Cell Sci.* **104,** 1217–1228 (1993).
15. Dibbayawan, T. P., Harper, J. D. I. & Marc, J. A γ-tubulin antibody against a plant peptide sequence localises to cell division-specific microtubule arrays and organelles in plants. *Micron* **32,** 671–678 (2001).
16. Ovechkina, Y. & Oakley, B. R. γ-tubulin in plant cells. *Methods Cell Biol.* **67,** 195–212 (2001).
17. Kumagai, F. *et al.* γ-tubulin distribution during cortical microtubule reorganization at the M/G1 interface in tobacco BY-2 cells. *Eur. J. Cell Biol.* **82,** 43–51 (2003).
18. Kumagai, F. *et al.* Fate of nascent microtubules organized at the M/G1 interface, as visualized by synchronized tobacco BY-2 cells stably expressing GFP-tubulin: time-sequence observations of the reorganization of cortical microtubules in living plant cells. *Plant Cell Physiol.* **42,** 723–732 (2001).
19. Sonobe, S. & Takahashi, S. Association of microtubules with the plasma-membrane of tobacco BY-2 cells *in vitro*. *Plant Cell Physiol.* **35,** 451–460 (1994).
20. Vesk, P. A., Vesk, M. & Gunning, B. E. S. Field emission scanning electron microscopy of microtubule arrays in higher plant cells. *Protoplasma* **195,** 168–182 (1996).
21. Hamada, T., Igarashi, H., Itoh, T. J., Shimmen, T. & Sonobe, S. Characterization of a 200 kDa microtubule-associated protein of tobacco BY-2 cells, a member of the XMAP215/MOR1 family. *Plant Cell Physiol.* **45,** 1233–1242 (2004).
22. Tian, G. W., Smith, D., Gluck, S. & Baskin, T. I. Higher plant cortical microtubule array analyzed in vitro in the presence of the cell wall. *Cell Motil. Cytoskel.* **57,** 26–36 (2004).
23. Dixit, R. & Cyr, R. Encounters between dynamic cortical microtubules promote ordering of the cortical array through angle-dependent modifications of microtubule behavior. *Plant Cell* **16,** 3274–3284 (2004).
24. Drykova, D. *et al.* Plant γ-tubulin interacts with αβ-tubulin dimers and forms membrane-associated complexes. *Plant Cell* **15,** 465–480 (2003).
25. Hoffman, J. C., Vaughn, K. C. & Joshi, H. C. Structural and immunocytochemical characterization of microtubule-organizing centers in pteridophyte spermatogenous cells. *Protoplasma* **179,** 46–60 (1994).
26. Bajer, A. S. & Mole-Bajer, J. Reorganization of microtubules in endosperm cells and cell fragments of the higher plant *Haemanthus in vivo*. *J. Cell Biol.* **102,** 263–281 (1986).
27. Palevitz, B. A. Microtubular fir-trees in mitotic spindles of onion roots. *Protoplasma* **142,** 74–78 (1988).
28. Smirnova, E. A. & Bajer, A. S. Microtubule converging centers and reorganization of the interphase cytoskeleton and the mitotic spindle in higher plant *Haemanthus*. *Cell Motil. Cytoskel.* **27,** 219–233 (1994).
29. Nagata, T., Nemoto, Y. & Hasezawa, S. Tobacco BY-2 cell-line as the Hela-cell in the cell biology of higher-plants. *Int. Rev. Cytol.* **132,** 1–30 (1992).
30. Ueda, K., Matsuyama, T. & Hashimoto, T. Visualization of microtubules in living cells of transgenic *Arabidopsis thaliana*. *Protoplasma* **206,** 201–206 (1999).
31. Horio, T. & Oakley, B. R. Expression of *Arabidopsis* γ-tubulin in fission yeast reveals conserved and novel functions of γ-tubulin. *Plant Physiol.* **133,** 1926–1934 (2003).
32. Walczak, C. E., Mitchison, T. J. & Desai, A. XKCM1: A *Xenopus* kinesin-related protein that regulates microtubule dynamics during mitotic spindle assembly. *Cell* **84,** 37–47 (1996).

nature cell biology



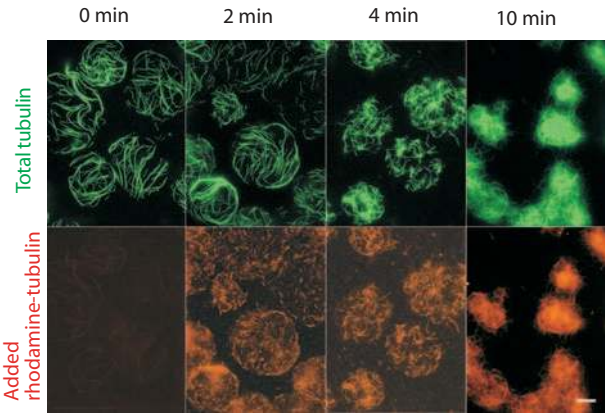


**Figure S1** Time course of microtubule assembly on tobacco protoplast ghosts detected by anti-α-tubulin (top panels, green) and added rhodamine-labeled brain tubulin (bottom panels, red). Scale bar, 10 μm.

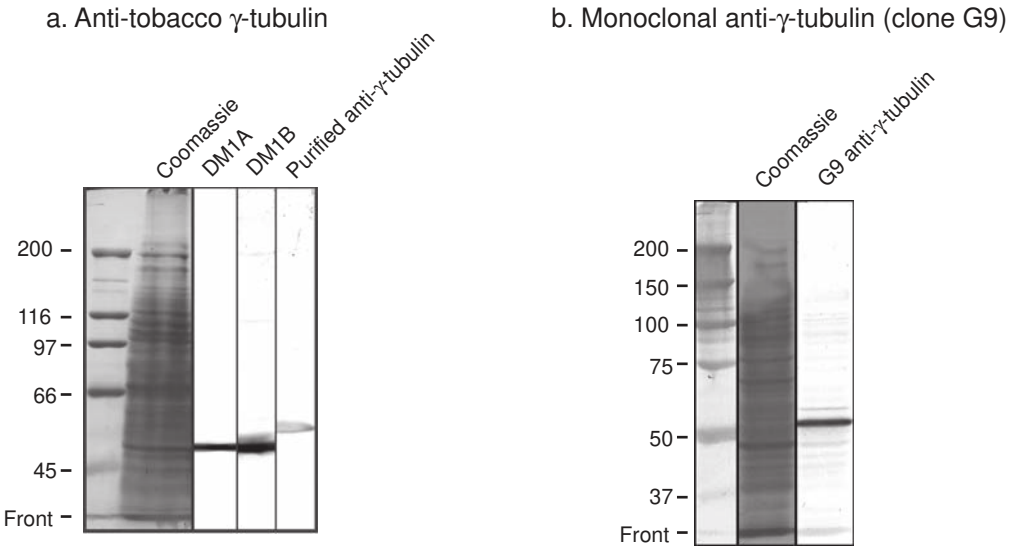


**Figure S2** Immunoblots showing specificity of anti-γ-tubulin used. (a) Antibody against carboxyl terminous of tobacco γ-tubulin. Crude proteins from tobacco BY-2 cells, run on a 7.5% polyacrylamide gel, were blotted onto a nitrocellulose membrane (Hybond-C super, Amersham) and the proteins were detected by Coomassie Brilliant Blue, anti-α-tubulin (clone DM1A, NeoMarkers, Union City, CA, USA) diluted at 1:100, anti-β-tubulin (clone DM1B, NeoMarkers) diluted at 1:10 and the adsorption purified anti-γ-tubulin diluted at 1:2000. The anti-γ-tubulin antibody detected only a single band at approximately 55 kDa. (b) Monoclonal antibody against fission yeast γ-tubulin (clone G9). Crude proteins were run on a 7.5% polyacrylamide gel, and detected by by Coomassie Brilliant Blue and monoclonal anti-γ-tubulin G9 diluted at 1: 1000.

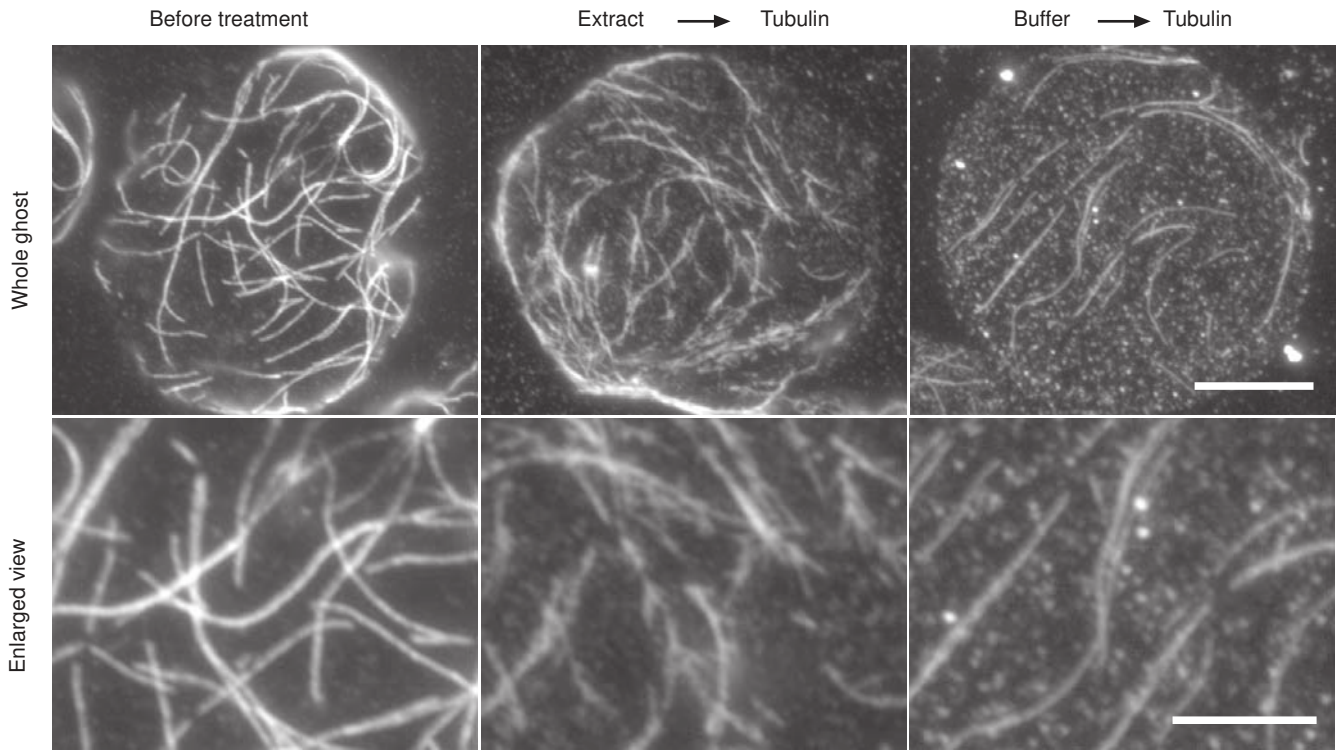


**Figure S3** A cytosolic extract with propyzamide give an ability of microtubule branching, upon addition of purified BY-2 tubulin, to microtubules on plasma membrane ghosts. Images of α-tubulin taken by a conventional fluorescence microscope. Plasma membrane ghosts were directly fixed (left panels) or fixed after the extract (with propyzamide) treatment followed by BY-2 tubulin treatment (center panels) or extraction buffer (with propyzamide) treatment followed by BY-2 tubulin treatment (right panels). Upper panels show whole ghosts, and lower panels show enlarged views of the corresponding upper panels. Scale bars, 10 μm (applied for upper panels) and 5 μm (applied for lower panels).

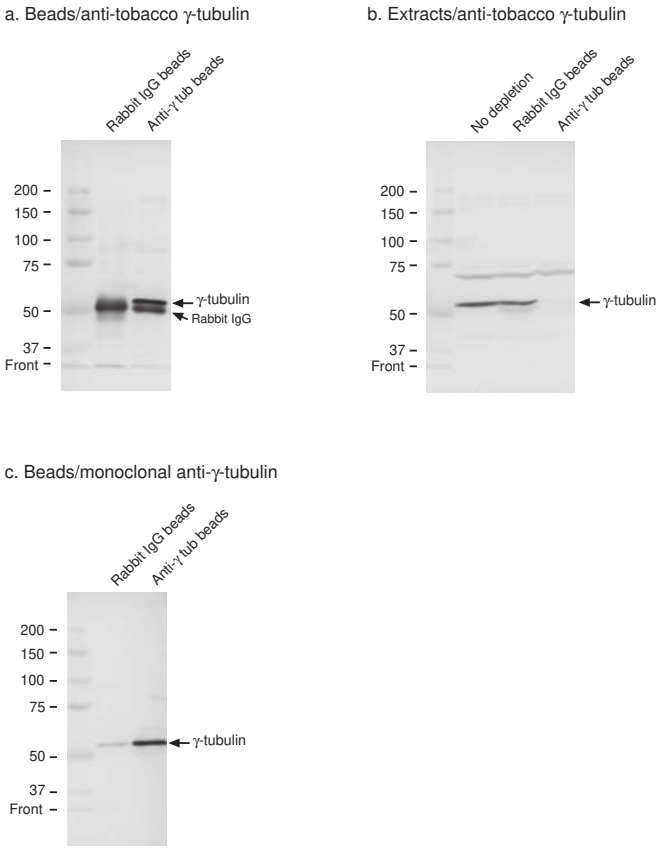


**Figure S4** Immunoblots showing specific immuno-depletion of γ-tubulin. (a) Proteins that bound to the beads were detected by unadsorbed (low-specificity version of) anti-γ-tubulin. Because anti-rabbit IgG was used as a secondary antibody, IgG bands are also detected. Note that a γ-tubulin band, running just above the IgG band, is detected in the sample from the anti-γ-tubulin beads. (b) Proteins of the extracts incubated with the beads analyzed in a. Proteins were detected by the unadsorbed anti-γ-tubulin. Bands of γ-tubulin (an arrow) and other proteins (below 75 kilodaltons) are detected in the blots, and a γ-tubulin band is depleted only in the lane from the anti-γ-tubulin beads. (c) Proteins that bound to rabbit IgG beads and anti-γ-tubulin beads detected by monoclonal anti-yeast γ-tubulin (clone G9). The intensity of γ-tubulin bands in the lane of anti-γ-tubulin beads is greatly increased, confirming that the anti-γ-tubulin beads react with γ-tubulin.

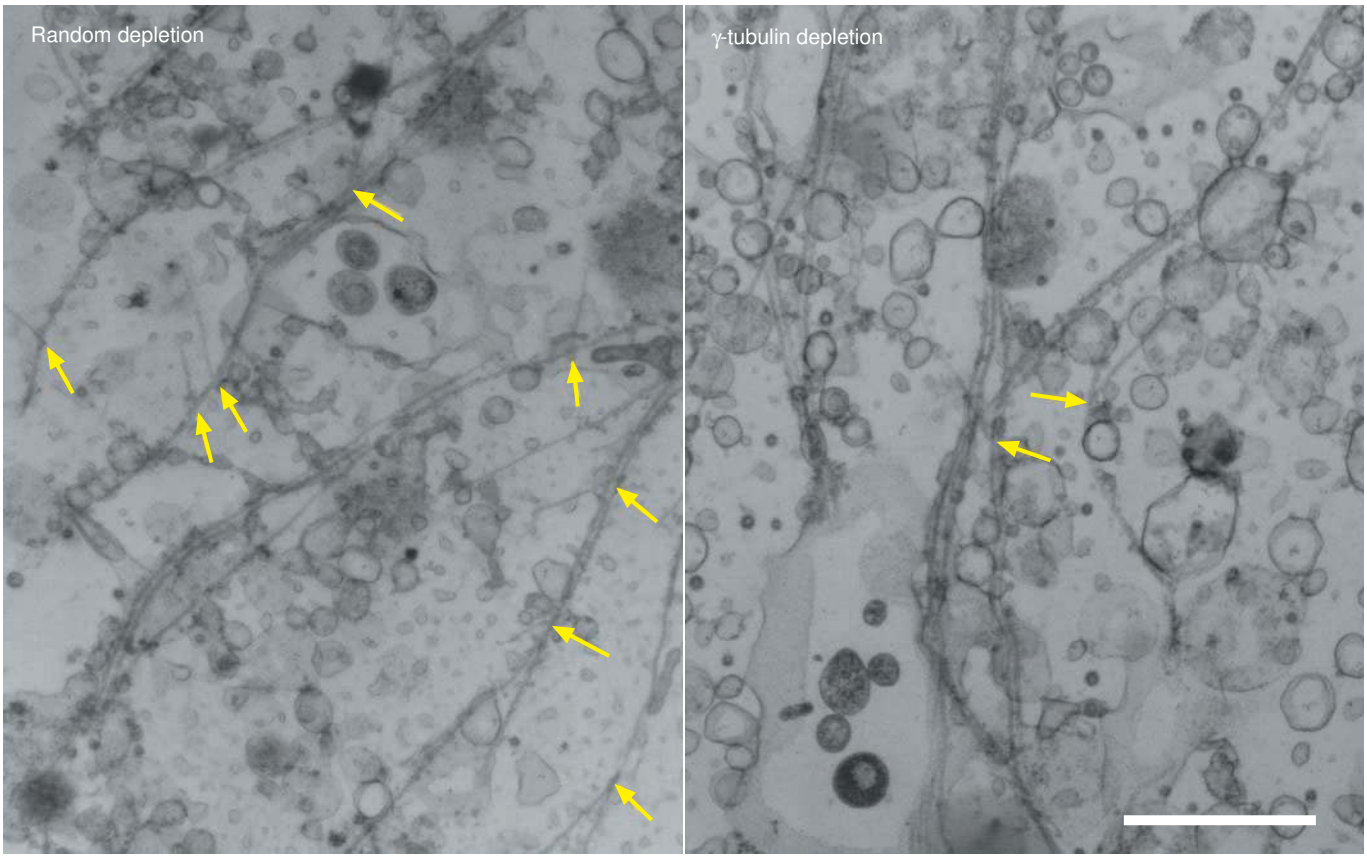


**Figure S5** Electron micrographs showing membrane ghosts prepared for quantification of branching in the sequential treatment system. Arrows indicate branching of microtubules. Scale bar, 1 μm.

**Table S1.** A significant fraction of immunogolds labels ends of microtubules on membrane ghosts of tobacco BY-2 cells.

| Antibody used | Number of gold particles | | |
|---|---|---|---|
| | End of microtubules[a] | Side of microtubules[b] | Others |
| Affinity-purified and membrane-adsorbed | 18 | 3 | 33 |
| Affinity-purified only | 22 | 22 | 61 |

[a] Including microtubule ends on the side of microtubules (branched microtubules).

[b] Excluding gold particles at branching.

**Movie 1** Initiation of cortical microtubules as branching in living tobacco BY-2 cells: Microtubules initiate as branches from pre-existing microtubules. A yellow arrow indicates the point of microtubule initiation. The original microtubule grows and shrinks before microtubule initiation, indicating that it is unlikely to be a bundle of microtubules. One second in the movie corresponds one minute of real time. Stills from this movie are shown in Fig. 1a.

**Movie 2** Initiation of cortical microtubules as branching in living tobacco BY-2 cells: Microtubules can initiate immediately following depolymerization of an original microtubule. A yellow arrow indicates the point of microtubule initiation. One second in the movie corresponds one minute of real time. Stills from this movie are shown in Fig. 1b.

**Movie 3** Initiation of cortical microtubules as branching in living tobacco BY-2 cells: The new microtubule often grows and shrinks while the original microtubule depolymerizes completely. A yellow arrow indicates the point of microtubule initiation. Once the original microtubule has gone, the newly formed microtubule appears as though the microtubule had initiated without a foundation microtubule. One second in the movie corresponds one minute of real time. Stills from this movie are shown in Fig. 1c.

**Movie 4** Initiation of cortical microtubules as branching in living leaf epidermal cells of *Arabidopsis thaliana*. Yellow arrows indicate the points of microtubule initiation. One second in the movie corresponds 15 seconds of real time.